 Cytometry 36:36–45 (1999)

Nine Color Eleven Parameter Immunophenotyping Using Three Laser Flow Cytometry

Martin Bigos,* Nicole Baumgarth, Gina C. Jager, Ometa C. Herman, Thomas Nozaki, Richard T. Stovel, David R. Parks, and Leonard A. Herzenberg

Department of Genetics, Stanford University School of Medicine, Stanford, California

Received 26 June 1998; Revision Received 17 December 1998; Accepted 22 December 1998

Background: This study describes a three laser flow cytometer, reagents, and software used to simultaneously evaluate nine distinct fluorescent parameters on one cell sample. We compare the quality of data obtained with (1) full software compensation and (2) the use of partial spectral compensation of selected pairs of parameters in analog hardware, in combination with final software compensation. An application characterizing low frequency murine B cell subpopulations is given.
Methods: The fluorochromes used are: fluorescein (FITC), phycoerythrin (PE), Cy5PE and Cy7PE, excited at 488 nm by an argon laser; Texas Red (TR), allophycocyanin (APC), and Cy7APC excited at 595 nm by a pumped dye laser; and cascade blue (CB) and cascade yellow (CY) excited at 407 nm by a violet-enhanced krypton laser. Custom additions to commercial electronics and an extended optical bench allow the measurement of these nine parameters plus forward and side scatter light signals.
Results: We find the use of partial analog compensation reduces the variation in the background staining levels introduced by the compensation process. Novel B cell populations with frequencies below 1% are characterized.
Conclusions: Nine color flow cytometry is capable of providing measurements with high information content. The choice of reagent-dye combinations and the ability to compensate in multi-parameter measurement space are crucial to obtaining satisfactory results. Cytometry 36:36–45, 1999. © 1999 Wiley-Liss, Inc.

Key terms: B lymphocytes; FACS; flow cytometry; multiparameter compensation

The introduction of cascade blue (CB) and cascade yellow (CY) (Molecular Probes, Inc., Eugene, OR) as violet-excited fluorochromes (2), and the use of Cy7 energy transfer conjugates with the phycobiliproteins phycoerythrin (Cy7PE) and allophycocyanin (Cy7APC) (13) has extended the number of useful fluorescence measurement parameters for immunophenotyping to nine. The use of eight of these simultaneously was demonstrated previously (2,12). We have now extended the instrumentation described therein to allow all nine of these fluorescent labels to be evaluated on each cell.

Capable instrumentation is only one aspect of performing complex multiparameter experiments. Two other, and equally important, aspects are reagent-dye selection and data analysis tools. In Roederer et al. (12) data were presented on two of the issues of reagent-dye selection: relative dye ''brightness'' and spectral interactions. Relative dye ''brightness'' is the ability of that dye to separate stained populations from background. Three different methods were presented to quantitate this attribute. Based on those results, the authors concluded that Cy5PE and APC are the two ''brightest'' dyes, followed by PE; TR and FITC are roughly equivalent, and CB and CY somewhat ''duller'' than the other dyes. The usefulness of these dyes, however, is also affected by their spectral interaction and the expression levels of the markers under investigation. In this report, we demonstrate how these aspects can be considered in the design of a set of reagent-dye combinations that identifies various murine splenic B-cell populations by incorporating all nine available fluorochromes.

Correcting for the spectral overlap between two dyes excited by the same laser to provide corrected estimates of the amount of signal produced by each dye was first introduced by Loken et al. (10). This system used subtraction of linear voltage pulses from the linear preamplification system of the electronics to implement the correction. Critical to this process is the requirement that the pulses produced by the electronic detection system (photomultiplier tube and current-to-voltage amplifier) for each dye are matched in shape and timing. Because flow instrumentation then and now uses the pulse height produced by the detection system as the measurement of the signal intensity, discrepancies of shape between subtracted pulses, which should yield a low or zero-level

Grant sponsor: NIH; Grant number: CA42509.
*Correspondence to: Martin Bigos, Beckman Center B007, Stanford University, Stanford, CA 94305–5318.
E-mail: bigos@stanford.edu

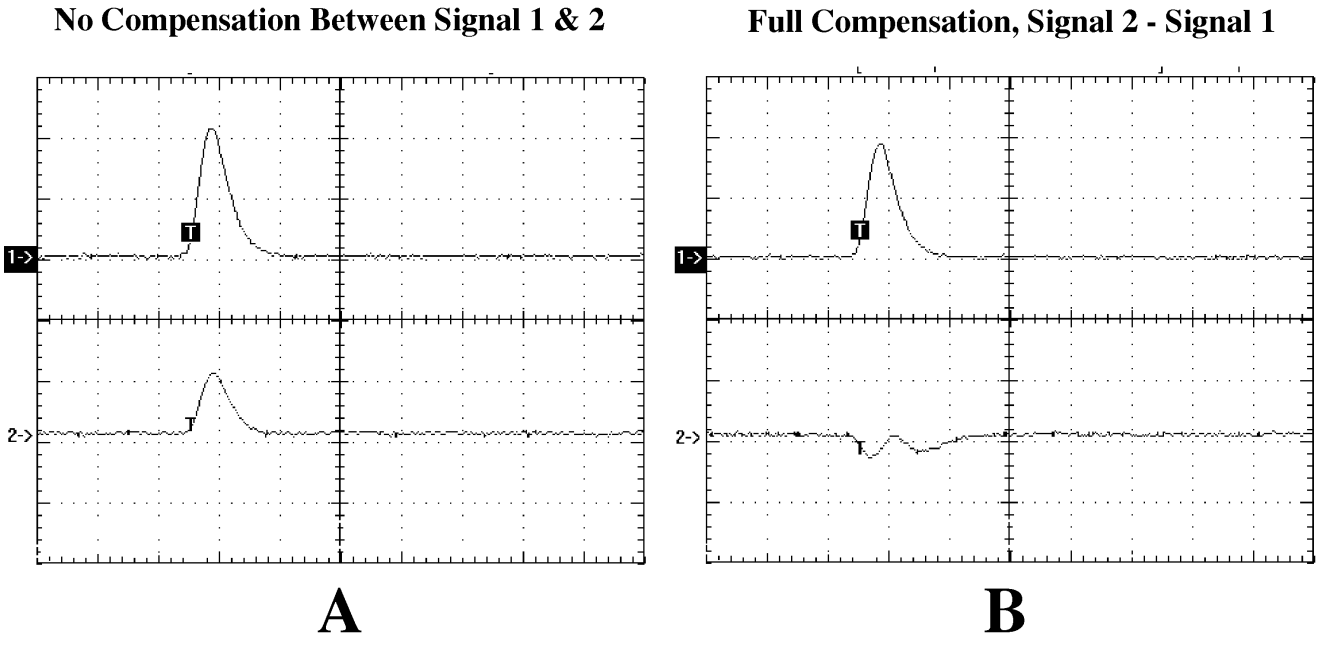

FIG. 1. Analog Pulse Subtraction. **A** and **B** are voltage pulses from the preamplifiers on the flow cytometer described in this paper generated by Rainbow Beads (Spherotech, Inc. Libertyville, IL). They are captured on a Textronix TDS 420 oscilloscope using Wavestar software (Textronix, Inc. Beaverton OR). Trace 1 shows the fluorescein signal, trace 2 shows the PE signal. The horizontal scale in both panels is 2 μsec. A: Vertical scale is 2 V, and no compensation is applied. B: Compensation has been used to subtract fluorescein from PE with the result shown as trace 2 (vertical scale 100 mv).

signal, will have residual peak(s) that do not correspond to the desired measurement (see Fig. 1). This error will tend to increase the variation of compensated signals, limiting the ability to measure low level signals above the autofluorescence background. This process of electronic peak subtraction is called analog compensation.

Mathematically, analog compensation can be modeled as a linear transformation of the ''signal'' vector space into the ''dye'' vector space, where the axes in that space represent the measurements of each dye alone. This model can easily be extended to any number of measurement parameters and implemented in software to correct flow data (as computer list mode files) for the spectral overlaps of more than two dyes; this was first mentioned by Roederer and Murphy (14) and further elaborated upon in Bagwell and Adams (3). The computations require that the list mode data be converted from log signal levels (which is used for the measurement of most immunofluorescence data) back to the linear domain to apply the model, then the results reconverted back to the log domain. However, a log amp is not a perfect device; our investigations (data not shown) have found that errors of $\pm 5\%$ are typical of log amp designs for flow cytometers, with the errors generally increasing at the bottom and top of the scale. Moreover, in most staining situations, the ''negative'' population signal is a mixture of cellular autofluorescence and non-specific staining. Thus, calculation errors and incomplete matching to the software model of the data deteriorates digitally compensated data.

Just as the software model can be extended as described above, the analog hardware can also be elaborated to correct more than two measurements. For multi-laser multi-fluorochrome configurations, a design that included delay lines to synchronize the pulses from the differently timed laser crossings and a large subtractive network to implement the myriad interactions among different dyes (see Table 1A) could be constructed. However, such a scheme has engineering difficulty meeting the requirement of matching pulse shapes and aligning them precisely in time, and would be difficult to expand as more measurement parameters are added.

Conceptually simpler would be to move the software model into the electronics by digitizing ''on the fly'' the linear pulses or peak heights of each event and processing them to obtain compensated log data that are then collected for analysis and/or used for sorting. Although modern microprocessors can easily handle the computation load, the engineering requirements in terms of bandwith and dynamic range of a system to digitize the linear signals have not yet been adequately met.

In this paper, we investigate a compromise system that uses analog compensation to partially compensate significant same laser spectral overlaps, followed by post-hoc software (digital) compensation. Using partial analog compensation minimizes the calculation errors of post-hoc software compensation while bringing the major same-laser spectral overlaps to a low level. By not attempting to fully compensate with analog electronics, the bias introduced by mismatched peak shapes is avoided. Applying software compensation to these signals minimizes the effects of calculation errors since the values subtracted are significantly smaller (see Table 1B) than those used for

Table 1
*Typical Spectral Spillover Matrices for Software Compensation**

Source	Measurement Parameter								
	FITC	PE	Cy5PE	TR	APC	Cy7APC	Cy7PE	CB	CY
A. Without partial analog compensation									
FITC	—	0.28	0.04	0	0	0	0.01	0	0.02
PE	0.02	—	0.18	0.03	0	0	0.02	0	0.02
Cy5PE	0	0.03	—	0.01	0.10	0.02	0.15	0	0
TR	0	0	0.01	—	0.12	0.02	0	0	0
APC	0	0	0.07	0.14	—	0.10	0.01	0	0
Cy7APC	0	0	0.05	0.25	0.68	—	0.14	0	0
Cy7PE	0	0.03	0.01	0	0	0.03	—	0	0
CB	0	0	0	0	0	0	0	—	0.07
CY	0.06	0.04	0.02	0	0	0	0.01	0.01	—
B. With partial analog compensation									
FITC	—	0	0	0	0	0	0	0	0.02
PE	0	—	0.03	0.03	0	0	0.01	0	0.02
Cy5PE	0	0.01	—	0	0.10	0.02	0.09	0	0
TR	0	0	0.01	—	0.02	0.01	0	0	0
APC	0	0	0.07	0.02	—	0.04	0	0	0
Cy7APC	0	0	0.05	0.17	0.57	—	0.14	0	0
Cy7PE	0	0.03	0	0	0	0.02	—	0	0
CB	0	0	0	0	0	0	0	—	0.01
CY	0.06	0.02	0.02	0	0	0	0.01	0	—

*__A__ is with no analog compensation; __B__ is with partial analog compensation as described in the text. For each row a sample singly stained with the source fluorochrome is run. The positive staining cells are selected and the median in each measurement channel calculated. Each row element is the ratio of the median in that measurement channel to the median in the source channel (spillover into source channel is not relevant and indicated by a dash). The inverse of this matrix, normalized so the position of the source medians remains constant, is the matrix used to calculate compensated parameters. The highlighted cells represent spillover values greater than 5%, which have been reduced by the use of partial analog compensation. Cross laser spillovers, in general, are not changed by the analog compensation used here.

pure digital compensation. In this study we show that this results in cleaner measurements on selected parameters than using software compensation alone.

However, there is at least one limitation in the compensation process that applies equally to all of the above possible methods: the quality of the underlying measurements itself. Compensation cannot decrease the variation in the original signals. Thus, in a log-log presentation of compensated data, visually the spread of a stained population relative to a spillover channel will generally be greater than the spread of the unstained cells. Moreover, the amount of light gathered for the measurements is an underlying determinant of how much the original variation may increase. In the red emission regions, the overall amount of light converted into electrical signals (photoelectrons) is lower that in the shorter wavelengths. Even though the staining intensity on the red-emitting parameters in general has a better signal/background ratio compared to the shorter wavelength-emitting dye, the absolute intensity is, in general, lower. This results in a greater uncertainty of measuring these signals, both in the primary measurement channels and channels with spectral overlap. In several cases, this is the limiting factor in how well compensation can be done independent of the method chosen. In the context of our study, while the use of partial analog followed by digital compensation results in a measurable decrease in the variation of the compensated signal compared to using digital compensation alone, the underlying variation in some measurement parameters due to the limited light available for the measurements obscures any advantage gained.

Data collection and analysis tools used for multiparameter experiments can help or hinder the process. Full annotation of data sets, including information regarding dye color, reagent, cell type, and any special conditions associated with the particular sample, is particularly useful for multiparameter analysis. A tool for constructing protocols, with which an entire cytometer run can be delineated in advance has been described previously (11) and has aided greatly in the management of complex multiparameter experiments. Furthermore, it is important to have analysis tools that can manage complex subset analysis, visualize data sets in different forms, and be able to handle large multiparameter data sets. A software program, FlowJo®, commercially available from Tree Star, Inc. (San Carlos, CA), has been designed over the past few years by our laboratory to fulfill these criteria.

We demonstrate here that with this system of hardware, software, and reagent system, nine fluorometric parameters can be used simultaneously, along with forward and side light scatters, for state of the art immunophenotyping. The data quality achieved is sufficient to characterize populations with both high and low ($<$1%) frequencies.

MATERIALS AND METHODS

Antibody Reagents

FITC-labeled monoclonal antibodies (mAbs) anti-CD21/CD35 (7G6), PE-labeled anti-CD24 (30F1), Cy5PE labeled

anti-CD3 (145–2C11), anti-CD5 (5.7) and anti-B220 (RB3–6B2), and purified, unconjugated anti-CD1 (3C11) were obtained from Pharmingen (San Diego, CA). Streptavidin-TR was obtained from Vector (Burlingame, CA). The following anti-murine mAbs were obtained by purifying serum-free tissue culture supernatants from hybridomas using protein G (Pharmacia, Piscataway, NJ) affinity chromatography: anti-B220 (RB3–6B2); anti-CD3 (145–2C11); anti-CD4 (G.K. 1.5); anti-CD8 (56.7.1); anti-F4/80 antigen (F4/80); anti-IgD (1126); anti-IgM (331); anti-CD43 (S7). The purified antibodies were conjugated to the following fluorochromes: CB: anti-CD3, anti-CD4, anti-CD8, anti-IgM, anti-B220, anti-F4/80; CY: anti-B220, anti-CD8; APC: anti-CD43, anti-IgM, anti-B220; Cy7APC: anti-IgM, anti-IgD; Cy7PE: anti-IgD; biotin: anti-CD1; PE: anti-CD5. Conditions of conjugations were exactly as described previously (6, 7, 12). Optimal staining concentrations were determined separately for each antibody-conjugate by titration on appropriate primary cells.

As controls for partial analog compensation individual samples of murine spleen cells were stained separately using each fluorochrome. To achieve optimal brightness some samples were stained with two or three antibodies conjugated to the same fluorochrome: FITC: anti-B220 and anti-IgM; PE: anti-IgM, anti-IgD and anti-B220; Cy5-PE: anti-B220; TR: anti-IgM, anti-IgD; APC: anti-IgM, anti-B220; Cy7APC: anti-IgM, anti-IgD; Cy7PE: anti-IgD; CB: anti-B220, anti-IgM; CY: anti-CD8. Partial analog compensation settings were chosen so that the spillover of the positively staining compensation control was reduced by at least half, when possible, without driving any related signals onto the measurement axes.

Murine spleen cells stained with anti-CD5 PE or TR and anti-CD3 Cy5PE were used to illustrate the visual comparison of partial analog compensation vs. no analog compensation.

Cell Staining and Analysis

Eight- to twelve-week-old BALB/c mice were taken from our breeding colony at the Research Animal Facility at Stanford University. Mice were sacrificed by cervical dislocation and single cell suspensions from spleens were obtained by gently disrupting the tissue between two glass-slides. Erythrocytes were lysed in ACK (9) buffer and remaining cells were resuspended at 2.5 x 10^7/ml in staining medium (deficient RPMI, 3% newborn calf serum, 1 mM EDTA, 20 μM azide). IgFcγR-receptors were blocked by incubating cells for 15 min on ice with the anti-FcγRII/III mAb 2.4.G2 (Pharmingen, San Diego, CA). For cell staining, equal volumes of (blocked) cells and antibody-cocktails, containing each antibody at its optimized concentration, were incubated in 96-well round-bottom plates on ice for 20 min. Cells were washed twice with staining medium and streptavidin-TR was added for a further 15 min on ice. Cells were washed twice, resuspended in staining medium containing propidium iodide at a final concentration of 0.25 μg/ml, and analyzed immediately. Data were collected by FACS-Desk (11) and analyzed using FlowJo® software (Tree Star, San Carlos, CA). In order to facilitate the elucidation of potentially small subpopulations, 100,000 events per sample were collected.

Cytometry Hardware

The hybrid flow cytometer, combining a modified FACStarPlus® optical bench (Becton Dickinson, San Jose CA) with MoFlo® (Cytomation, Inc., Fort Collins, CO) and custom electronics, has been described in detail (12). Figure 2 is revised from Roederer et al. (12) to show the nine color detector configuration. The 407-nm emission arm was modified by adding a beam splitter and emission filter for CY, and by reversing the position of the CB detector and the (formerly spare and now) CY detector.

The overall layout of the electronics was left unchanged from Roederer et al. (12) and is not reproduced here. However, three modifications were made to different parts of the system. First, the MoFlo® electronics console was upgraded by the manufacturer to use a 32-word data frame. This makes it possible to add ADC boards (now 6 in the console) to process eleven measurement parameters (two light scatter signals and nine colors). Second, some of our custom electronics were changed. In particular, the preamplifiers were replaced with a set of computer-controlled compensating preamplifiers, and the preamplifiers are connected to non-rectifying logarithmic amplifiers (8) whose outputs feed linear inputs of the MoFlo® electronics. This allows pair-wise analog compensation between the following fluorochromes: FITC and PE, PE and Cy5PE, PE and Cy7PE, Cy5PE and Cy7PE, TR and APC, APC and Cy7APC, and CB and CY. Third, minor modifications were made to our instrument control and monitoring software to accommodate the above hardware changes.

RESULTS

Reagents

All direct antibody conjugates can be used to stain cells simultaneously. However, we observed that a high concentration of CB or CY can lead to unspecific binding of the other violet-light excited fluorochrome to the stained cells, resulting in false double-positive staining. To avoid this problem, we currently use only one of the two violet-light excited flurochromes conjugated during the first staining step and stain with the other reagent in a second step, if applicable, together with the streptavidin conjugate.

Compensation Between 407-nm and 488-nm Excited Parameters

Both FITC and PE are slightly excited by the 407-nm laser line, and CY is slightly excited by the 488-nm laser line. Thus, FITC and PE show a small but measurable spillover into the CY measurement channel and CY has a similar spillover into the FITC and PE measurement channels (see Table 1A). CB and CY also have small spectral overlaps with each other in this configuration. Digital compensation is effective at removing this low level of specral overlap (data not shown), while the combination of partial analog compensation and post-hoc software

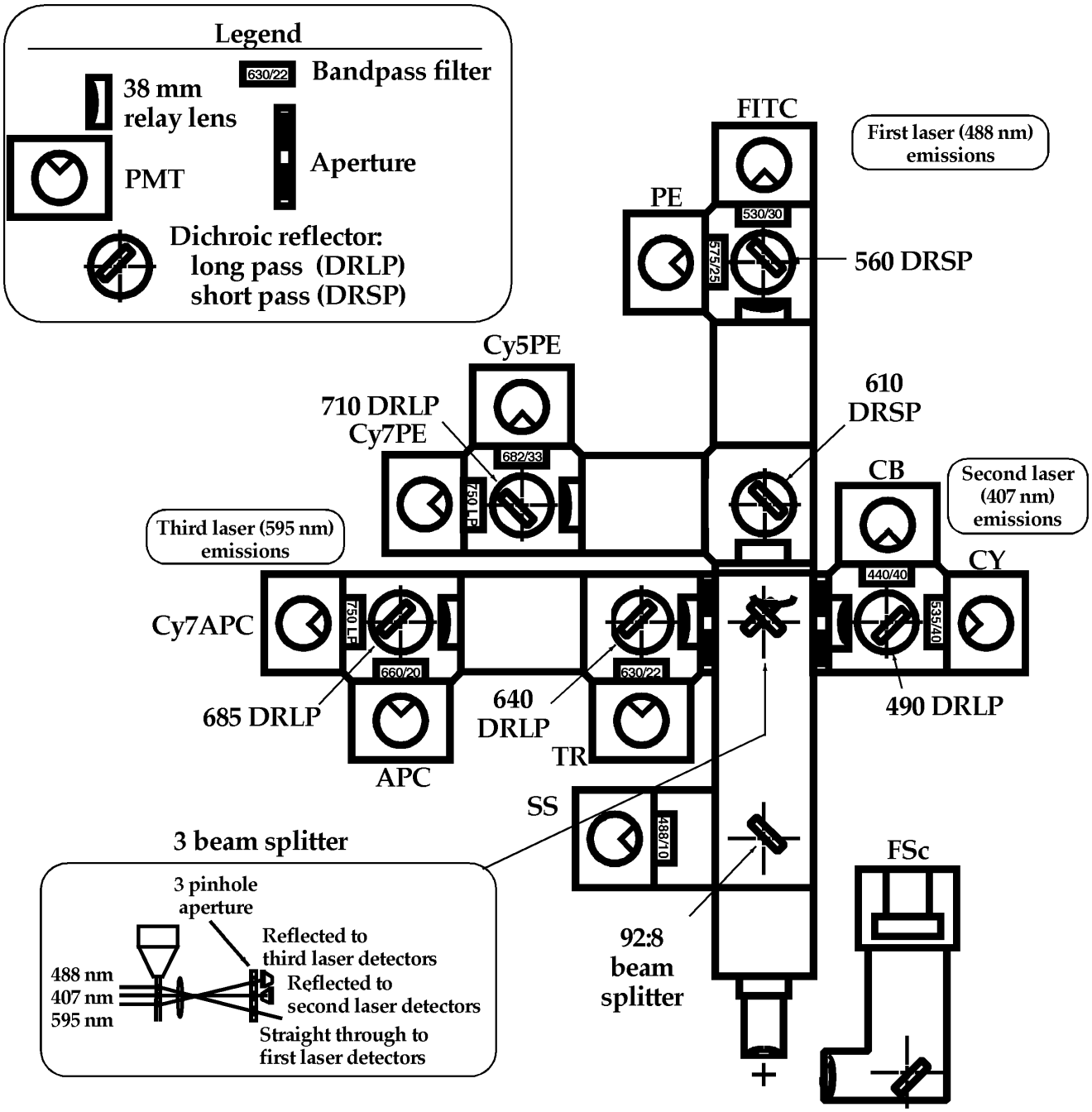

FIG. 2. Optical Layout and Filters for Nine Color Measurements. This block diagram shows the optical layout on the modified FACStarPlus® bench that is in use for nine color eleven parameter measurements. Relay lenses are used on the extended pathways to refocus the emission onto the PMT detectors. Filters and beam splitters that are not standard Becton Dickinson parts were obtained from either Chroma Technology Corp, Brattleboro VT, or Omega Optical, Brattleboro, VT. Note the change in position of the CB detector when CY is added, compared to Figure 2 in Roederer et al. (12).

compensation is effective at removing the overlap of CB into CY (see Table 2 and Fig. 3).

Using Partial Analog Compensation

We next determined whether the use of partial analog compensation can improve the compensation results. Poor compensation will result in a broader range of the compensated signal on a spillover channel. That is, a poor signal, compared to a better one, will simultaneously have more events on the reagent axis as well as events further off the axis. Thus, compensated signals with lower introduced variation will allow one to better discriminate low-level staining from negative events in multicolor measurements.

Table 2
*Typical Effects of Partial Analog Compensation on Signal Measurement**

Measurement	Spectral spillover (no analog comp.)	Spectral spillover (partial analog comp.)	Light level on spillover channel (cv) (%)	Reduction in variation on spillover channel (%)
FITC → PE	0.29	0.01	5.5	15
PE → Cy5PE	0.18	0.03	9.3	18
Cy5PE → Cy7PE	0.15	0.09	9.6	15
TR → APC	0.12	0.02	15	15
APC → TR	0.14	0.02	14	8
APC → Cy7APC	0.10	0.04	21	7
Cy7APC → APC	0.68	0.57	29	0
CB → CY	0.07	0.01	7.1	11

*The compensation controls were run with no analog compensation and partial analog compensation as described. Forward and side light scatter gates were set to eliminate dead cells and debris. The spectral spillover columns are copied from Table 1. The ''Reduction in variation on spillover'' resulting from partial analog compensation is measured on the spillover channel, calculated using the difference between the 75th and 50th percentiles of the gated cells in the samples described, without and with the use of partial analog compensation. The ''light level on spillover'' is the CV of a narrow slice around the median of positively staining cells calculated on the spillover channel.

A common statistical metric for comparing the range of a measurement is the difference between a high and low percentile, say the 75th and 25th percentiles. However, this metric will not be usable here because half or more of the events of the unstained population are at lowest measurable signal level (i.e., ''on the axis''). To avoid this artifact, we choose the somewhat ad-hoc metric of the difference between the 75th and 50th percentiles on the spillover parameters.. This allows us to numerically compare the variation in the two methods of compensation.

The boxes highlighted in Table 1A show the same laser spectral overlaps that are significant and can be reduced using partial analog compensation, as shown in the corresponding spectral overlaps in Table 1B. Table 2 list these results from Table 1 and the computed changes along with our ad-hoc metric. Also listed is the coefficient of variation (CV) on the spillover channel of a uniform population of positively staining cells on the source channel. This number reflects the uncertainty of measurements due to statistical variation (photon statistics) on both the source and spillover channels, with more uncertainty resulting in a larger value.

Table 2 shows that partial analog compensation followed by digital compensation results in reduction of the variation of signal in the spillover channel compared to using digital compensation alone. This improvement is correlated, with one exception, with the light level estimates provided. There is less relation to the original size of the spillover or the amount of spillover reduction provided by analog compensation, as long as both are non-trivial. We are not sure why the 4th row of this table (TR-APC) does not fit this pattern, and plan to investigate this further.

Figure 3 shows the underlying data sets for Table 2 displayed as contour maps. The horizontal lines help visualize the reduction in variation by showing a decrease in the extreme values of the stained populations. Plots corresponding to the last two rows of Table 2 are not shown; there is no variation change in Cy7APC-stained population as measured on APC, and the variation changes for CB-stained populations do not noticeably affect the extreme values of them.

Application to Immunophenotyping of Murine Splenic B-Cells

To identify potentially novel B-cell subsets in the spleen, 9-color staining cocktails were devised that included a series of surface markers that are known to stain B-cell subpopulations. Figure 4 shows the analysis of one such cocktail on one cell sample. After live cell gating by Forward Scatter-Side Scatter profile and propidium iodide exclusion (data not shown), cells were selected for their expression of the pan-B cell marker B220. To exclude the small number of T-cells that express this marker, and to exclude macrophages that might interfere with the analysis, cells were also stained with several anti-T-cell markers (anti CD3, anti-CD4, anti-CD8) and the macrophages marker F4/80.

Non-T-cells expressing B220 were then separated into IgM^{low} IgD^{hi} and IgM^{hi} IgD^{low} B cells. The majority of IgD^{hi} IgM^{low} cells (gate E, Fig. 4A) expressed all characteristics of follicular B cells: $CD21^{int.}$ $CD43^{-}$ $CD1^{low}$ $CD24^{low}$ $CD5^{-}$. However, like the cells within gates A and D, a subpopulation of cells expressed high levels of CD1 (shown as expression levels above indicated bar in plot), consistent with a previous report that demonstrated that a subset of follicular B cells expressed high levels of CD1 (1).

Analysis of CD43 and CD21 revealed three subpopulation among the IgM^{hi} IgD^{low} cells: $CD21^{-}CD43^{-}$ (gate B) $CD21^{int.}$ $CD43^{+}$ (gate A) and $CD21^{hi}$ $CD43^{-}$ (gate C). Cells within gate B were characterized as a homogeneous population of $CD24^{hi}$, $CD1^{low}$ and $CD5^{-}$ cells, consistent with their being immature B-cells (1,5). Cells in gate C also appeared homogenous, expressing the following phenotype: $CD1^{hi}$ $CD24^{int.}$ $CD5^{-}$. This phenotype is associated with marginal zone B-cells (1). The majority of cells within gate A was $CD24^{int.}$ $CD1^{low}$ and $CD5^{+}$. Therefore, the phenotype of this cell population is that of B-1 cells, representing about 0.3% of all events acquired. The

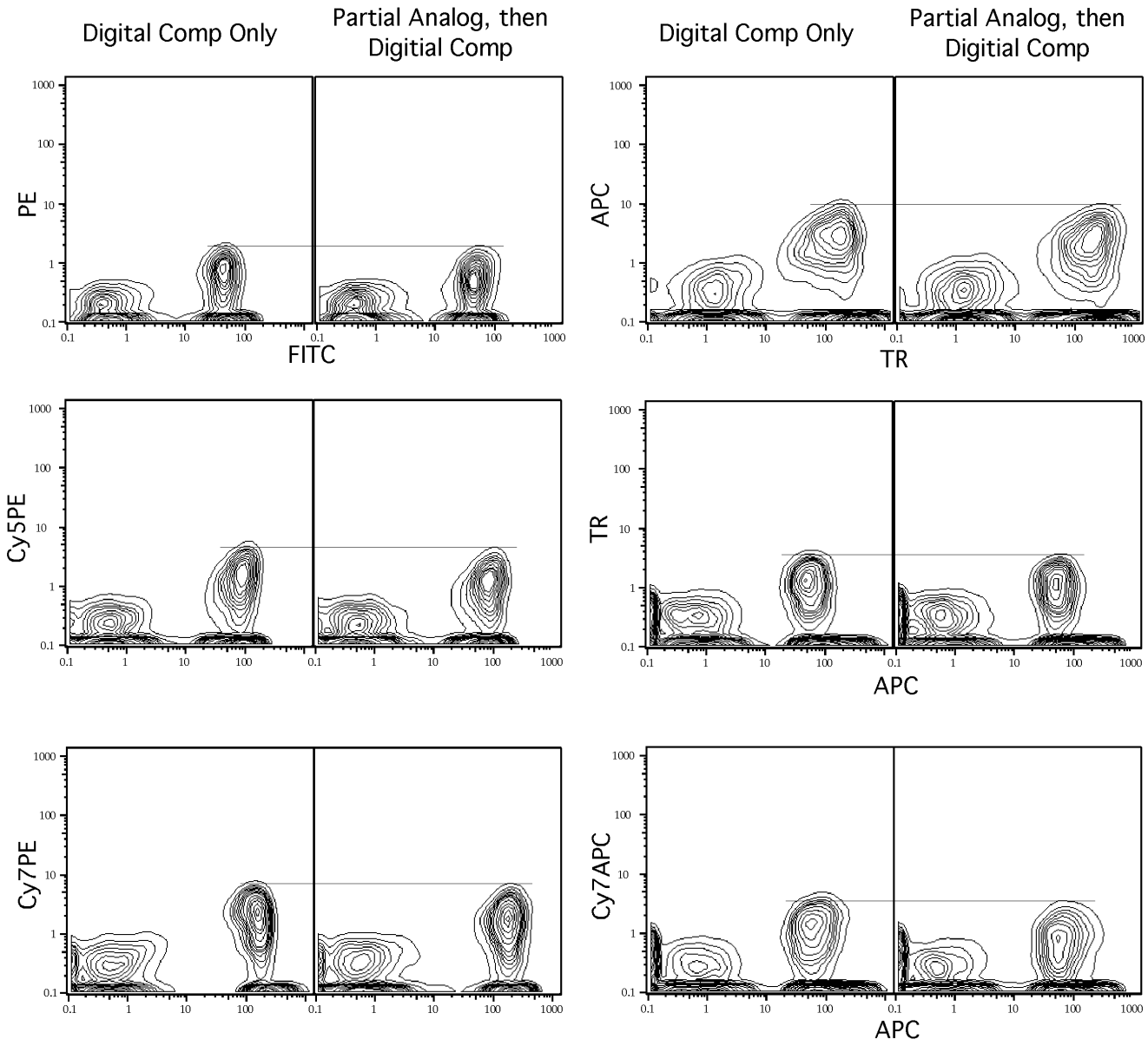

FIG. 3. Typical influence of compensation on data quality. Spleen cells from BALB/c mice were stained were stained as compensation controls as described in the text. Forward and side light scatter gates were set to eliminate dead cells and debris. The six pairs of contour plots (5% probability contours) correspond to the first six lines in Table 2. In each pair the left plot is generated using software (digital) compensation only, and the right plot is generated from data to which analog compensation was applied, followed by software compensation. The horizontal line on each pair is drawn at the lowest contour level of the positivily stained population in the right plot.

hallmark of B-1 cells is their expression of CD5 and CD43, which is believed to be restricted to this subset (1,5).

Interestingly, a second $CD5^+$ B cell population was identified which also expressed high levels of CD43, but belonged within the IgM^{low} IgD^{hi} B cell subset (D), associated with follicular B cells. Cells within gate D were similar to the B-1 cells in their expression of CD43 and CD21, however, they expressed less CD24 than B-1 cells, as measured by their mean fluorescent intensities (MFI) of 7.9 vs. 14.2. Furthermore, they also expressed lower levels of CD5 (MFI 11 vs. 22, respectively). This population of cells with the phenotype IgD^{hi} IgM^{low} $CD43^+$ $CD24^{int.}$ $CD1^{low}$ $CD5^+$ represents 0.6% of cells within the original sample, and does not correspond to any previously published B-cell subpopulation.

To confirm that this population was not artificially created by the gates set to separate IgM^{hi} IgD^{low} and IgM^{hi} IgD^{low} cells, we determined the expression of IgM vs. IgD on $B220^+$ $CD43^+$ and $B220^+$ $CD43^-$ cells. As shown in Figure 5, $B220^+$ $CD21^{int.}$ $CD43^+$ cells are heterogeneous in their expression of IgM and IgD. In comparison to the $CD43^-$ cells, a higher relative frequency of $CD43^+$ cells expresses IgM^{hi} IgD^{low}, presumably B-1 cells. However, a significant number of cells in this gate expresses IgM^{low}

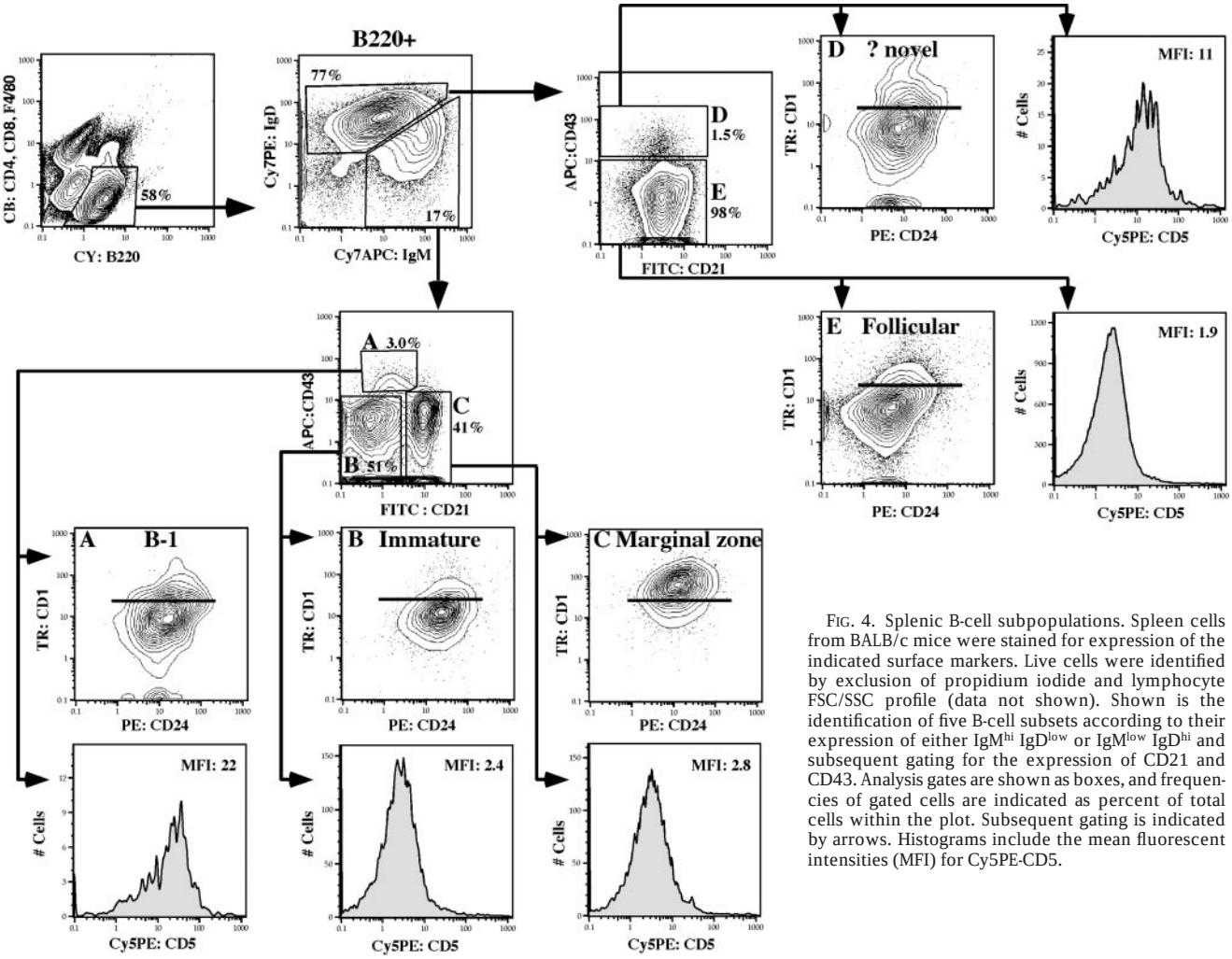

FIG. 4. Splenic B-cell subpopulations. Spleen cells from BALB/c mice were stained for expression of the indicated surface markers. Live cells were identified by exclusion of propidium iodide and lymphocyte FSC/SSC profile (data not shown). Shown is the identification of five B-cell subsets according to their expression of either IgM^{hi} IgD^{low} or IgM^{low} IgD^{hi} and subsequent gating for the expression of CD21 and CD43. Analysis gates are shown as boxes, and frequencies of gated cells are indicated as percent of total cells within the plot. Subsequent gating is indicated by arrows. Histograms include the mean fluorescent intensities (MFI) for Cy5PE-CD5.

IgD^{hi}, therefore constituting the second population of $CD43^+$ cells, identified as $CD5^+$ conventional B-cells.

Therefore, we identified, using nine distinct conjugates on one sample, five discrete B-cell subpopulations, at least three of which showed further heterogeneity with regard to their expression of CD1 and CD24.

DISCUSSION

We demonstrate in this report the feasibility of using nine dyes along with two light scatter signals for immunophenotype analysis. Using antibodies conjugated to four different fluorochromes excited at 488 nm, three excited at 595 nm, and two excited at 407 nm, we further demonstrate the unprecedented capabilities of this flow cytometric assay by identifying with a single data collection a total of five distinct murine B-cell subpopulations in the spleen of normal mice, one of which has not been described before.

For the simultaneous analysis of multiple cell surface markers, careful choice of the dyes to be used with each antibody is critical. The first consideration is whether a certain marker is expressed at high or low levels on the cells of interest. A suitable candidate dye should be chosen based on (1) dye ''brightness'' and (2) spectral interactions. Spectral interactions have to be considered, as spectral overlap and the compensation process can degrade the measurement, especially when the signal size, overlaps, and amount of adjustments required are large. For example, CD5 is expressed highly on T-cells, but is expressed at low levels on certain B-cell subsets. Very few conjugates will resolve these cells from the background. ''Bright'' dyes in our system are Cy5PE and APC. Considerable overlap exists between APC and Cy7APC, and other dyes such as Cy5PE and TR also interfere with the APC measurement. As a result of these overlaps, the APC negative cells have a relatively broad distribution, which potentially can make the resolution of dimly staining populations difficult. In contrast, less spillover into the Cy5PE channel was observed, and Cy5PE proved to be a useful dye in our configuration for measuring the low expression of CD5 on certain B cell subsets. Thus, for the analysis of a novel surface marker for which the particular characteristics in expression levels are not clear, it is important to choose stains and combination of stains that

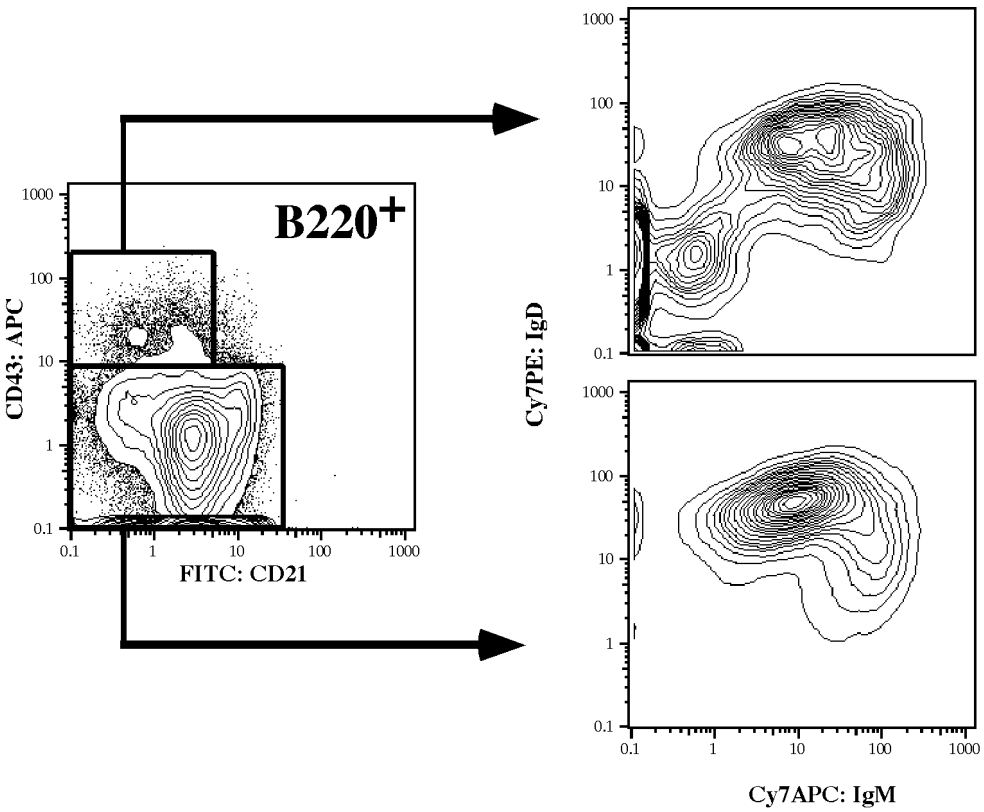

FIG. 5. CD43 expressing B cells are heterogeneous. $B220^{+}CD3^{-}$ $CD4^{-}$ $CD8^{-}$ $F4/80^{-}$ cells obtained as shown in Figure 4 were gated as indicated into $CD43^{+}$ and $CD43^{-}$ cells and analyzed for their expression of IgM and IgD. Shown are 5% probability contour plots.

have minimal influence on the channels in which the markers of interest are measured.

At the other end of the ''brightness'' spectrum are the dyes CB and CY. These dyes produce a relatively small signal in relation to typical autofluorescence background, so that antibody conjugates have to be chosen that identify markers that are expressed uniformly at relatively high levels on cell subsets. An example is given in Figure 4, in which distinct B- and T-cell markers were chosen for use with the Krypton laser excited dyes. On the other hand, these dyes have very little measurement overlap from other fluorochromes, so that even low frequency populations of cells can be identified distinctively with these dyes.

In the case of FITC, the overlap from the other dyes range from small to negligible. Even though FITC is only a moderately ''bright'' dye, it is useful for distinguishing even relative small differences in the expression levels of a given cell surface marker. An example for this is provided in Figure 4, in which the expression of the complement receptor CD21 is studied on B-cells. As shown, the expression levels of this marker vary only about 10- to 20-fold among the different B-cell subsets, however, good separation was achieved and enabled the identification of three B-cell subsets among the IgM^{hi} IgD^{low} cells.

The usefulness of some dyes can be further increased by using a biotin-avidin system. In the example shown in Figure 4, ''bright'' CD1 staining was achieved using biotin-CD1 together with Streptavidin-TR.

In the process of making these choices, it is important to confirm the staining patterns for each of the reagent-dye combinations by measuring the marker of interest in the presence and absence of each of the other stains in the antibody cocktail. When compensation is applied, ideally the expression levels, as measured by mean fluorescent intensity of the populations of interest, should be identical in the presence or absence of each of the other reagents. For certain dye combinations, such as APC and Cy7APC, this is very difficult to achieve. When a population with high expression levels is stained with a conjugate using one of these dyes, the background levels measured for the other reagent most often will also increase somewhat. Carrying out the control measurements described above will facilitate the distinction of weak positive staining from background.

It is also important to note that the figures of merit for dye brightness given in Roederer et al. (12), upon which the above considerations are based, are not absolute, but relative both to the dyes and the instrument. Optical and flow geometry, the level of the background on various measurement parameters, and excitation conditions can have a strong effect on the ordering of the various dyes For example, among the three 488 nm excited dyes, FITC, PE, and Cy5PE, PE is the ''brightest'' on a FACScan® (Becton Dickinson, San Jose, CA) by the three criteria used in Roederer et al. (12) (data not shown), while Cy5PE is the ''brightest'' on our jet-in-air sorter. Thus, until appropriate inter-instrument standards and calibrations exist, one

should evaluate the dyes in use in their own particular configuration before making final determinations regarding their ''brightness.''

Partial analog compensation followed by digital compensation in post-hoc software, reduces the variation of cell distributions than software compensation used alone. Visually this can result in small improvements in the separation of subpopulations depending upon the reagent-dye combinations used. However, the improvement is not great enough to overcome unsuitable reagent combinations or the inherent variation due to low light (i.e., photoelectron) levels on some measurement parameters, hence the process of reagent choice described above must be carefully carried out for satisfactory results.

After a certain staining combination has been established and the staining patterns verified with the appropriate controls, the introduction of one new marker in a tested reagent combination becomes easy. It is then that the power of multicolor analysis becomes apparent. The expression levels of the new marker among the previously identified cell subpopulations can be determined within one sample. In the example shown in Figure 4A, a novel B cell subpopulation was identified not by introducing a novel marker, but by the ability to apply simultaneously a number of known surface makers. Expression of CD5 and CD43 was thought to be restricted to B-1 cells, which comprise only a small fraction of the B cells in the spleen of adult mice and are thought to represent a separate B-cell lineage from follicular B-cells (15). However, the data shown here suggest that a small percentage of B-cells, which show all the hallmarks of follicular B-cells, namely their expression of IgM^{low} IgD^{hi} $CD21^{int}$ $CD24^{int}$ $CD1^{low}$, can also express these two markers. Further differences between conventional CD5-expressing B-cells and B-1 cells were seen with regard to the levels of CD5 that are expressed by these different cells. The finding of conventional CD5-expressing B-cells is in agreement with earlier in vitro studies that demonstrated that conventional B-cells can express CD5 under certain stimulation conditions (4). Further work is needed to confirm the origin of the two CD5 expressing B-cell populations in the spleens of normal mice, to determine whether they indeed belong to separate B-cell lineages.

Although our hardware involved considerable in-house development, at least one manufacturer (Cytomation, Inc.) can supply a system with similar multicolor measurement capability, although without analog compensation. We expect the other major manufacturers, as they introduce new systems and retrofit their old ones, to provide similar capability for making these simultaneous measurements. Flow cytometric measurements on cells are used not only for phenotypic analysis, but also for various functional studies, such as Ca^{++}-flux analysis, activation marker expression, gene expression, and the identification of type and frequency of cytokines produced by a given cell population. The development of multicolor flow cytometric systems, such as the one described in this study, provides the tools for combining complex functional and phenotypic measurements on heterogeneous cell populations for their analysis immediately ex vivo. The system described here can, therefore, enhance the quality and the feasibility of many cell biological studies.

ACKNOWLEDGMENTS

We thank the reviewers for their careful reading and helpful comments, which have improved the presentation of this paper.

LITERATURE CITED

1. Amano M, Baumgarth N, Dick M, Herzenberg LA, Herzenberg LA. CD1 expression defines subsets of follicular and marginal zone B cells in the spleen: B2m-dependent and independent forms. J Immunol 1998;161:1710–1717.
2. Anderson MT, Baumgarth N, Haugland RP, Gerstein RM, Tjioe IT, Herzenberg LA, Herzenberg LA. Pairs of violet-light excited fluorochromes for flow cytometric analysis. Cytometry 1998;33:435–444.
3. Bagwell CB, Adams EG. Fluorescence spectral overlap compensation for any number of flow cytometry parameters. Ann NY Acad Sci 1993;677:167–184.
4. Bandyopadhyay RS, Teutsch MR, Wortis HH. Activation of B-cells by sIgM cross-linking induces accumulation of CD5 mRNA. Curr Top Microbiol Immunol 1995;194:219–228.
5. Best CG, Kemp JD, Waldschmidt TJ. Murine B-cell subsets defined by CD23. In: Methods: a companion to methods in enzymology. San Diego: Academic Press, Inc.; 1995. p 3–10.
6. Hardy RR. Purification and characterization of monoclonal antibodies. In: Weir DM, editor. Handbook of experimental immunology. Oxford: Blackwell Scientific Publications; 1986. p 13.11.
7. Hardy RR. Purification and coupling of fluorescent proteins for use in flow cytometry. In: Weir DM, editor. Handbook of experimental immunology. Oxford: Blackwell Scientific Publications; 1986. p 31.31.
8. Hiebert RD, Sweet RG. Electronics for flow cytometers and sorters. In: Van Dilla M, editor. Flow cytometry: instrumentation and data analysis. London: Academic Press; 1985. p 129–161.
9. Lalor PA, Stall AM, Adams S, Herzenberg LA. Permanent alteration of the murine Ly-1 B repertoire due to selective depletion of Ly-1 B cells in neonatal animals. Eur J Immunol 1989;19:501–506.
10. Loken MR, Parks DR, Herzenberg LA. Two-color immunofluorescence using a flourescence-activated cell sorter. J Hist Cytol 1977;25:899–907.
11. Moore WA, Kautz RA: Data analysis in flow cytometry. In: Weir DM, Herzenberg LA, Blackwell CM, Herzenberg LA, editors. Handbook of experimental immunology, 4 ed. Edinburgh: Blackwell Scientific Publications; 1986. p 30.31–30.11.
12. Roederer M, DeRosa S, Gerstein R, Anderson MT, Bigos M, Stovel RT, Nozaki T, Parks DR, Herzenberg LA, Herzenberg LA. 8 color, 10-parameter flow cytometry to elucidate complex leukocyte heterogeneity. Cytometry 1997;29:328–339.
13. Roederer M, Kantor AB, Parks DR, Herzenberg LA. Cy7PE and Cy7APC: bright new probes for immunofluorescence. Cytometry 1996;24:191–197.
14. Roederer M, Murphy R. Cell-by-cell autofluorescence correction for low signal-to-noise systems: application to epidermal growth factor endocytosis by 3T3 fibroblasts. Cytometry 1986;7:558–565.
15. Wells SM, Kantor AB, Stall AM. CD43 (S7) expression identifies peripheral B cell subsets. J Immunol 1994;153:5503–5515.